

Finite-temperature phase transitions in quasi-two-dimensional spin-1 Bose gases

Ville Pietilä,^{1,2} Tapio P. Simula,^{3,4} and Mikko Möttönen^{1,2,5}

¹*Department of Applied Physics/COMP, Aalto University, P. O. Box 15100, FI-00076 AALTO, Finland*

²*Australian Research Council Centre of Excellence for Quantum Computer Technology,
School of Electrical Engineering & Telecommunications,
University of New South Wales, Sydney NSW 2052, Australia*

³*Department of Physics, Okayama University, Okayama 700-8530, Japan*

⁴*School of Physics, Monash University, Victoria 3800, Australia*

⁵*Low Temperature Laboratory, Aalto University, P. O. Box 13500, FI-00076 AALTO, Finland*

Recently, the Berezinskii-Kosterlitz-Thouless transition was found to be mediated by half-quantum vortices (HQVs) in two-dimensional (2D) antiferromagnetic Bose gases [Phys. Rev. Lett. **97**, 120406 (2006)]. We study the thermal activation of HQVs in the experimentally relevant trapped quasi-2D system and find a crossover temperature at which free HQVs proliferate at the center of the trap. Above the crossover temperature, we observe transitions corresponding to the onset of a coherent condensate and a quasicondensate, and discuss the absence of a fragmented condensate.

PACS numbers: 03.75.Lm, 05.30.Jp, 03.75.Mn, 64.70.Tg

I. INTRODUCTION

The dimension of the underlying space has a profound impact on the existence of long-range order and phase transitions in a given system. In two-dimensional (2D) systems the long-range order and spontaneous symmetry breaking are forbidden [1–3]; however, 2D systems can exhibit a quasi-long-range order with algebraically decaying correlations [4–7]. The disordered high-temperature phase and the algebraically ordered low-temperature phase are separated by a topological phase transition corresponding to the unbinding of pairs of vortices and antivortices. This phase transition is referred to as the Berezinskii-Kosterlitz-Thouless (BKT) transition [4, 6]. However, experimentally relevant examples often display additional features due to the finite-size effects [8], and in the trapped ultracold atomic gases where the BKT transition has recently been studied [9–13], the inhomogeneous density of the gas renders the superfluid state and the coherence properties qualitatively different from those of the bulk systems [13–15].

Spinor Bose gases [16–18] are especially interesting as they can in principle combine magnetic ordering, formation of a condensed component, and superfluidity. Due to the interplay of these competing orders, the antiferromagnetic spin-1 Bose gas is expected to host various exotic phenomena such as fragmented condensates [19] and fractionalized topological objects [20, 21] that are usually absent in the single-component systems. For example, a half-quantum vortex (HQV) confined to a spin defect occurs in spin nematic condensates [20, 22] and it has recently been created using Raman-detuned laser pulses [23]. In homogeneous 2D optical lattices, proliferation of HQVs in spin-1 Bose systems due to thermal fluctuations has been predicted [24, 25], and the superfluid transition in two dimensions was found to be mediated by HQVs [26]. In ferromagnetic spinor condensates, HQVs have shown to give rise to intriguing magnetization dynamics [27]. Fractional vortices and the related BKT transitions have also been discussed in the context of ³He [28] and different nonconventional superconductors [29–31]. Recently, HQVs have been

observed in exciton-polariton condensates [32].

While the connection between superfluidity and Bose-Einstein condensation is relatively well understood in the single-component Bose systems [4, 6, 9–15], the existence of spin degree of freedom in spinor Bose gases renders the relation between superfluidity and long-range order more complicated and far less studied. In particular, the existence and the nature of the possible condensed component is not yet known in two dimensions. The recent experimental interest in spinor Bose gases with antiferromagnetic interactions [33, 34], advances in the evaporative cooling of optically trapped atoms [35], and the nondestructive imaging of the local magnetization of spin-1 Bose gases [36, 37] suggest that the experimental realization of the finite-temperature phase transitions in quasi-2D spinor Bose gases may be possible in the near future. Hence, we study the activation of different topological defects associated with the superfluid transition and determine the different degenerate components of quasi-2D antiferromagnetic spin-1 Bose gases. Our approach is valid in the regime where the thermal fluctuations are dominant and our results suggest that in this region, the condensate state is nonfragmented.

II. FORMALISM

To study the behavior of a spinor Bose gas near the critical region we use a classical field (*c* field) to describe the highly occupied low-energy modes and a quantum field for the thermal modes with low occupation [38]. Previously, this approach has been successfully applied in studies of the BKT transition in scalar Bose gases [9, 14, 15, 39] as well as to predict other properties of dilute scalar Bose gases [40–46]. The coherence properties of spinor Bose condensates at finite temperatures have recently been studied using an alternative formulation of the *c*-field method [47].

The dynamics of the *c* field can be described by the pro-

jected Gross-Pitaevskii equation (PGPE)

$$i\hbar \partial_t \vec{\Psi}_C = \hat{h}_0 \vec{\Psi}_C + \mathcal{P} \{ c_0 |\vec{\Psi}_C|^2 \vec{\Psi}_C + c_2 (\vec{\Psi}_C^\dagger \mathcal{F} \vec{\Psi}_C) \cdot \mathcal{F} \vec{\Psi}_C \}, \quad (1)$$

which generalizes the usual spinor Gross-Pitaevskii equation [16, 17]. In the PGPE, \mathcal{F} denotes a vector of spin-1 matrices and \mathcal{P} implements a projection into the subspace of the classical modes [38]. The c field in Eq. (1) is written in the basis consisting of the Zeeman substates such that $\vec{\Psi}_C = (\psi_{C,\alpha})$, $\alpha = 1, 0, -1$. The single-particle operator \hat{h}_0 is given by

$$\hat{h}_0 = -\frac{\hbar^2}{2m} \nabla^2 + \frac{m}{2} (\omega_\perp^2 r_\perp^2 + \omega_z^2 z^2).$$

The coupling constants c_0 and c_2 are given by $c_0 = 4\pi\hbar^2(a_0 + 2a_2)/3m$ and $c_2 = 4\pi\hbar^2(a_2 - a_0)/3m$, where m is the atomic mass and a_0 and a_2 are the s -wave scattering lengths in the total hyperfine spin channels $F = 0$ and $F = 2$, respectively [17]. Antiferromagnetic interactions imply $c_2 > 0$, and we take $a_0 = 46a_B$, $a_2 = 52a_B$, and $m = 3.86 \times 10^{-26}$ kg, according to ^{23}Na [17]. The Bohr radius is denoted by a_B .

In the quasi-2D limit, $\omega_\perp \ll \omega_z$ and we choose $\omega_z = 200 \times \omega_\perp$. Harmonic oscillator lengths in axial and transverse directions are denoted by $a_z = \sqrt{\hbar/m\omega_z}$ and $a_\perp = \sqrt{\hbar/m\omega_\perp}$. The scattering can be treated as three-dimensional as long as $a_0, a_2 \ll a_z$ [48, 49]. This condition is satisfied with the previous choice of ω_z and ω_\perp if we take $\omega_\perp = 2\pi \times 10$ Hz which is in the realm of the current experiments. Since we consider a quasi-2D situation, the PGPE and all c fields are defined in a 3D space. The spatial vector of the 3D space is denoted by \mathbf{r} and \mathbf{r}_\perp is a 2D vector in the $x - y$ plane. Summation over repeated indices is implied.

In the PGPE, the c-field region \mathcal{C} is defined by the energy cutoff ε_{cut} such that $\mathcal{C} = \{n | \varepsilon_n \leq \varepsilon_{\text{cut}}\}$, corresponding to the spectrum of the single-particle operator \hat{h}_0 . The c fields in Eq. (1) can be expressed in terms of the eigenstates of \hat{h}_0

$$\psi_{C,\alpha}(\mathbf{r}) = \sum_{n \in \mathcal{C}} c_{\alpha,n} \varphi_n(\mathbf{r}). \quad (2)$$

The PGPE corresponds to a microcanonical system in which the stationary probability distributions are determined by the total energy of system, and the temperature and the chemical potential are computed as ensemble averages. We use the ergodic hypothesis to replace all ensemble averages with the corresponding time averages. Using the ergodic hypothesis, thermodynamical quantities such as the temperature and the chemical potential can be computed dynamically [38, 41, 50].

Let us briefly discuss how to generalize the single-component calculation of the temperature and the chemical potential [38, 41, 50] to the spin-1 case. The PGPE (1) arises from the Hamiltonian

$$H_C = \int d\mathbf{r} [\vec{\Psi}_C^\dagger \hat{h}_0 \vec{\Psi}_C + \frac{c_0}{2} |\vec{\Psi}_C|^4 + \frac{c_2}{2} (\vec{\Psi}_C^\dagger \mathcal{F} \vec{\Psi}_C)^2] \quad (3)$$

for which the canonical coordinates can be defined such that

$$Q_{\alpha,n} = \frac{1}{\sqrt{2\varepsilon_n}} (c_{\alpha,n}^* + c_{\alpha,n}) \quad \text{and} \quad P_{\alpha,n} = i\sqrt{\frac{\varepsilon_n}{2}} (c_{\alpha,n}^* - c_{\alpha,n}), \quad (4)$$

where $c_{\alpha,n}$ are the coefficients in Eq. (2). The canonical coordinates are collectively denoted by $\Gamma = \{Q_{\alpha,n}, P_{\alpha,n}\}$. According to a general theorem [51], the temperature can be calculated as

$$\frac{1}{k_B T} \equiv \left(\frac{\partial S}{\partial E} \right)_N = \langle \mathcal{D} \cdot \mathbf{X}_T(\Gamma) \rangle, \quad (5)$$

where the first identity is the standard definition of the temperature of a microcanonical system. The derivative operator $\mathcal{D} = \{e_n \partial / \partial \Gamma_n\}$, determined by the coefficients $\{e_n\}$, and the vector field \mathbf{X}_T can be chosen freely as long as they satisfy the conditions [38, 41, 50]

$$\mathcal{D}H_C \cdot \mathbf{X}_T = 1 \quad \text{and} \quad \mathcal{D}N_C \cdot \mathbf{X}_T = 0, \quad (6)$$

where $N_C = \int d\mathbf{r} |\vec{\Psi}_C|^2$ is the total number of the c-field atoms. The vector field \mathbf{X}_T satisfying the above constraints is given by [41, 50]

$$\mathbf{X}_T = \frac{\mathcal{D}H_C - \lambda_N \mathcal{D}N_C}{|\mathcal{D}H_C|^2 - \lambda_N (\mathcal{D}N_C \cdot \mathcal{D}H_C)}, \quad (7)$$

with $\lambda_N = (\mathcal{D}N_C \cdot \mathcal{D}H_C) / |\mathcal{D}N_C|^2$. Straightforward choices for the vector operator \mathcal{D} are $\mathcal{D}_P = \{0, \partial_{P_n}\}$ and $\mathcal{D}_Q = \{\partial_{Q_n}, 0\}$ [50]. The temperature is independent of the choice the derivative \mathcal{D} , and the two different choices serve also as a check for the numerical implementation. The average in Eq. (5) is computed as a corresponding time average.

The preceding formulation can be applied when the only conserved quantity is the total particle number N_C . In the present case, also the angular momentum is conserved. Transforming to the coordinate system with zero total angular momentum, the angular momentum conservation does not appear in Eqs. (6) and (7) [50, 52]. For spinor Bose gases, the conservation of the total magnetization also needs to be taken into account. In the antiferromagnetic case, however, the total magnetization is zero and can be neglected in light of the previous argument. Using the definition $\mu/k_B T = -(\partial S / \partial N)_E$, also the chemical potential μ can be computed by interchanging the roles of H_C and N_C . Computationally efficient formulation for the different terms in Eqs. (5) – (7) proceeds in an analogous way to Ref. [50].

The number of atoms outside the c-field region can be computed self-consistently using the Hartree-Fock-Popov (HFP) approximation [9, 14, 38, 53]. The full field operator containing the c-field part $\psi_{C,\alpha}$ and the incoherent part $\delta\hat{\phi}_{I,\alpha}$ is denoted by $\hat{\Phi}_\alpha = \psi_{C,\alpha} + \delta\hat{\phi}_{I,\alpha}$. We assume that terms such as $\langle \psi_{C,\alpha} \delta\hat{\phi}_{I,\beta} \rangle$, $\langle \psi_{C,\alpha} \delta\hat{\phi}_{I,\beta}^\dagger \rangle$, and all their complex conjugates

vanish. This leads to the HFP single-particle energies [53]

$$\varepsilon_+(\mathbf{k}, \mathbf{r}) = \frac{\hbar^2 \mathbf{k}^2}{2m} + V_{\text{tr}}(\mathbf{r}) - \mu + c_0(n_+ + n_-) + c_2(2n_+ + n_0 - n_-), \quad (8a)$$

$$\varepsilon_0(\mathbf{k}, \mathbf{r}) = \frac{\hbar^2 \mathbf{k}^2}{2m} + V_{\text{tr}}(\mathbf{r}) - \mu + c_0(n_+ + n_0) + c_2(n_+ + n_-), \quad (8b)$$

$$\varepsilon_-(\mathbf{k}, \mathbf{r}) = \frac{\hbar^2 \mathbf{k}^2}{2m} + V_{\text{tr}}(\mathbf{r}) - \mu + c_0(n_+ + n_-) + c_2(2n_- + n_0 - n_+), \quad (8c)$$

where $n_\alpha = \langle \hat{n}_\alpha \rangle = |\psi_{c,\alpha}|^2 + \langle \delta \hat{\phi}_{I,\alpha}^\dagger \delta \hat{\phi}_{I,\alpha} \rangle$ and $n = \langle \hat{n} \rangle = n_+ + n_0 + n_-$. The occupation number $n_\alpha^{(I)} = \langle \delta \hat{\phi}_{I,\alpha}^\dagger \delta \hat{\phi}_{I,\alpha} \rangle$ for the incoherent atoms can be computed from the Bose-Einstein distribution using the semiclassical integral in a 3D phase space

$$n_\alpha^{(I)}(\mathbf{r}) = \int \frac{d\mathbf{k}}{(2\pi)^3} \frac{1}{e^{\varepsilon_\alpha(\mathbf{k}, \mathbf{r})/k_B T} - 1}. \quad (9)$$

The quasi-2D nature of the system is taken into account by treating the axial modes discretely in the semiclassical integral [14]. The energy cutoff ε_{cut} introduces a spatially dependent low-energy cutoff to the semiclassical integral (9) (see Ref. [14]).

III. TOPOLOGICAL DEFECTS AND NEMATIC ORDER

The c field in Eq. (1) is written in the z -quantized basis $\vec{\Psi} = (\psi_\alpha)$, $\alpha = -1, 0, 1$, but the nematic properties of anti-ferromagnetic Bose gases are more conveniently expressed in the Cartesian representation [16, 54] $\vec{\Psi} = (\psi_a)$, $a = x, y, z$. The transformation is given by $\psi_x = (\psi_1 - \psi_{-1})/\sqrt{2}$, $\psi_y = i(\psi_1 + \psi_{-1})/\sqrt{2}$, and $\psi_z = \psi_0$ and the nematic order is described by the spin quadrupole moment [54] $Q_{ab}^{(s)} = (\psi_a^* \psi_b + \psi_b^* \psi_a)/(2|\vec{\Psi}|^2)$. In general, $Q^{(s)}$ has three distinct nonzero eigenvalues and the local magnetic axis \hat{n} is defined as the eigenvector associated with the largest eigenvalue. For $\psi_z \equiv 0$, the magnetic axis is confined into the $x - y$ plane and we refer to such case as the ‘‘in-plane’’ nematic.

In the polar phase which corresponds to identically vanishing local spin [17], the Cartesian representation gives $\vec{\Psi} = \sqrt{\varrho} e^{i\theta} \hat{n}$ and the HQV corresponds to a defect where both θ and \hat{n} have a π winding about the core of the defect. Furthermore, the polar phase allows also the existence of skyrmions which have finite energy and are characterized by the second homotopy group of the order parameter space. In the Appendix, explicit expressions for the HQVs and skyrmions are presented. The polar phase has a local \mathbb{Z}_2 invariance corresponding to $(\theta, \hat{n}) \rightarrow (\theta + \pi, -\hat{n})$ [21, 22, 55]. This implies that defects with opposite topological charges cannot be distinguished and therefore we define the sign of the HQV

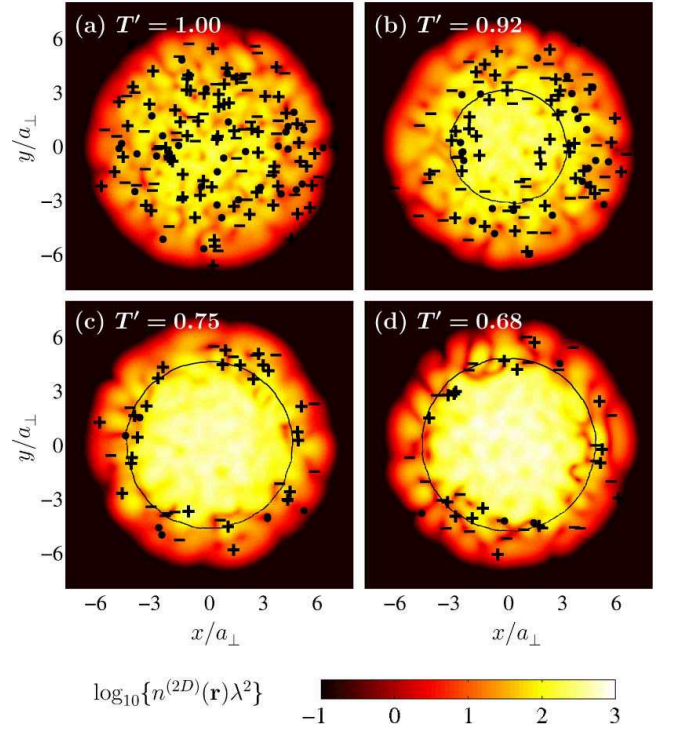


Figure 1: (Color online) Instantaneous density of the c-field atoms corresponding to the out-of-plane nematic phase. Half-quantum vortices and antivortices are denoted by black + and - symbols, respectively. Skyrmions are marked with black dots. The black line denotes the boundary outside which $n_c/\bar{n}_{\text{tot}} < 0.1$, where n_c is the condensate density, and \bar{n}_{tot} is the average total density of the c-field atoms. The thermal wavelength is denoted by λ . In the instantaneous density, the z -dependence is integrated out. The temperature is given with respect to the critical temperature of the corresponding quasi-2D ideal Bose gas (see Section III).

from the polarization of the vortex core [22]. Furthermore, we do not distinguish between skyrmions with opposite winding numbers [56]. An example of the thermally activated HQVs and skyrmions is shown in Fig. 1 where the instantaneous z -integrated densities of the c-field atoms at different temperatures are depicted.

We consider two phases, the in-plane nematic with $\bar{n}_{c,+1} = \bar{n}_{c,-1}$ and $\bar{n}_{c,0} \equiv 0$ and an ‘‘out-of-plane’’ nematic with $\bar{n}_{c,+1} \approx \bar{n}_{c,0} \approx \bar{n}_{c,-1} = 0.33 \pm 0.06$. Here $\bar{n}_{c,\alpha}$ refers to the average number of c-field atoms in the component α , divided by the total number of atoms N_C in the c-field region. The average numbers $\bar{n}_{c,\alpha}$ corresponding to the different data points in Figs. 2 and 3 vary between the aforementioned limits. In both cases, we take $N_C = 15000$ and choose the energy cutoff as $\varepsilon_{\text{cut}} = 126 \hbar \omega_\perp$ ($\varepsilon_{\text{cut}} = 122 \hbar \omega_\perp$) for the in-plane (out-of-plane) nematic. For these values of the cutoff energy, only the lowest axial mode becomes populated and the c-field region is in the ground state with respect to motion in the z direction. Nevertheless, the incoherent region atoms typically occupy several axial modes.

As indicated in Ref. [25], the in-plane nematic phase arises in the spin-1 case as a result of a large negative quadratic Zee-

man shift (for a discussion how the negative shift is physically realized, see Refs. [25, 57]). In the case of the PGPE, elimination of the $\alpha = 0$ component corresponds to leaving the $\alpha = 0$ component empty in the initial state. The quadratic Zeeman shift can be absorbed in the single-particle energies since it is the same constant for the $\alpha = \pm 1$ components. This allows us to treat the in-plane and out-of-plane cases at equal footing, assuming only that the Zeeman shift is large enough to eliminate the $\alpha = 0$ component at the relevant temperatures.

The ensemble averages are calculated as corresponding time averages such that the system is allowed to thermalize for period $50 \times 2\pi/\omega_\perp$ and the time average is computed from 1250 equally spaced samples. The sampling interval is $50 \times 2\pi/\omega_\perp$ ($100 \times 2\pi/\omega_\perp$) for the in-plane (out-of-plane) nematic phase. The randomized initial states are taken from the polar phase corresponding to zero magnetization. Otherwise the numerical implementation follows the description of Refs. [38, 58]. In the HFP calculation for the in-plane nematic, we assume that there are no thermal atoms in the $\alpha = 0$ component.

We keep the cutoff energy fixed, which causes the total number of atoms N_{tot} to increase with increasing temperature. To accommodate to the varying atom number, we scale the temperature by the critical temperature T_0 of a quasi-2D ideal Bose gas corresponding to the same total particle number [15]. For the in-plane (out-of-plane) nematic phase, T_0 corresponds to the critical temperature of two (three) independent ideal Bose gases. For the ideal Bose gas, there is a standard relation between the temperature and the occupation number of the thermal component [15, 59]

$$N(T) = \sum_{n \neq 0} \frac{1}{e^{(\varepsilon_n - \varepsilon_0)/k_B T} - 1}, \quad (10)$$

where ε_n are the 3D harmonic oscillator energies. We calculate T_0 numerically by solving the equation $N(T_0) = \gamma N_{\text{tot}}$ where $\gamma = 1/2$ for the in-plane phase and $\gamma = 1/3$ for the out-of-plane phase. We denote the reduced temperatures by T' and the bare temperatures by T . In experiments, a precise control of the total atom number at different temperatures is difficult and hence the approach presented here is likely to describe well the realistic experimental conditions.

IV. CONDENSATE AND QUASICONDENSATE

The existence and the nature of the condensate and the quasicondensate components in antiferromagnetic Bose gases are particularly interesting due to the possibility of a fragmented condensate at zero temperature [19]. Since the fragmentation in this case corresponds to the condensation of composite bosons to the $|\mathbf{k} = 0\rangle$ state in the momentum space, it seems that also the fragmented condensate is destroyed by the thermal fluctuations in a homogeneous 2D system. In addition, the thermally activated HQVs render the single-mode approximation used in Refs. [19, 60] invalid and it is a nontrivial question whether the fragmented condensate can exist in 2D at finite temperatures. In this work, the presence of a signif-

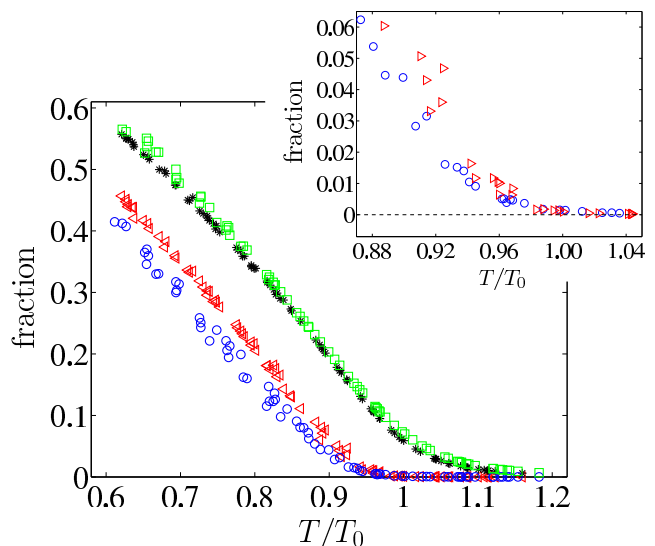


Figure 2: (Color online) Condensate fraction N_0/N_{tot} for the in-plane nematic (blue circles) and the out-of-plane nematic (red triangles) phases as a function of the reduced temperature. The quasicondensate fraction is almost identical for the in-plane nematic (green squares) and out-of-plane nematic (black asterisks) phases. Note that the definition of the reduced temperature differs between the in-plane and the out-of-plane phases (see text for details). (Inset) The condensate fraction near the temperature corresponding to the onset of the condensate. The dashed line is a guide for the eye.

icant thermal component renders a direct comparison to the zero temperature single mode calculations difficult.

In the homogeneous 2D case, algebraic order is expected in the paired state corresponding to $\Theta = \hat{\Phi}_0 \hat{\Phi}_0 - 2\hat{\Phi}_{+1} \hat{\Phi}_{-1}$ [26] and inspection of the correlation function $\langle \Theta^\dagger(\mathbf{r}'_\perp) \Theta(\mathbf{r}_\perp) \rangle$ could shed light on the superfluid properties of the antiferromagnetic spin-1 Bose gases. In this work, we are interested in the existence and the nature of a condensed component in spin-1 superfluids and consider therefore the one-body density matrix $\rho^{(1)}(\mathbf{r}\alpha; \mathbf{r}'\beta) = \langle \hat{\Phi}_\beta^\dagger(\mathbf{r}') \hat{\Phi}_\alpha(\mathbf{r}) \rangle$ which can be sampled using the time averaging. Under the previous assumptions it separates into two parts containing the c-field part and the incoherent part. At low temperatures, we find that $\rho^{(1)}$ has only a single macroscopic eigenvalue N_0 and we refer to N_0/N_{tot} by the generic name “condensate fraction.”

Above the critical temperature of condensation, $\rho^{(1)}$ has several large eigenvalues although their fraction of N_{tot} becomes vanishingly small. This thermally induced fragmentation [60] is, however, different from the fragmentation due to the ordering in the spin sector. Our results seem to be consistent with the idea of a hierarchy of transition temperatures such that the formation of a coherent condensate is followed by ordering in the spin sector, leading potentially to a fragmented condensate in the zero-temperature limit [60]. The condensate fraction is shown in Fig. 2 as a function of the reduced temperature $T' = T/T_0$.

For the scalar Bose gas, the quasicondensate component can be defined using the correlation function $\mathcal{C}(\mathbf{r}_\perp) = 2\langle \hat{\phi}^\dagger(\mathbf{r}_\perp) \hat{\phi}(\mathbf{r}_\perp) \rangle^2 - \langle [\hat{\phi}^\dagger(\mathbf{r}_\perp) \hat{\phi}(\mathbf{r}_\perp)]^2 \rangle$ [15, 61], describing

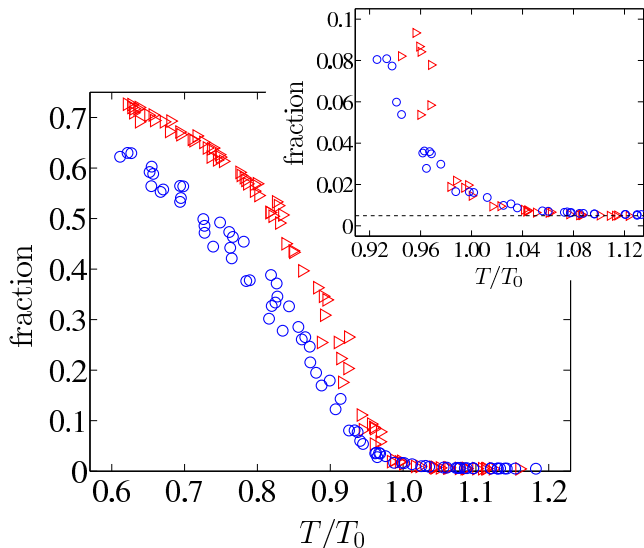


Figure 3: (Color online) The largest eigenvalue of the one-body density matrix (N_0) normalized by the number of the c-field atoms (N_C) as a function of the reduced temperature. The inset shows the same quantity zoomed to the temperatures corresponding to the onset of a large eigenvalue. The out-of-plane nematic is denoted by (red) triangles, and (blue) circles correspond to the in-plane nematic phase. The dashed line is a guide for the eye.

the part of the system with reduced total density fluctuations. In the spinor case, we may consider an equivalent quantity $\mathcal{C}(\mathbf{r}_\perp) = 2\langle\hat{\Phi}_\alpha^\dagger(\mathbf{r}_\perp)\hat{\Phi}_\alpha(\mathbf{r}_\perp)\rangle^2 - \langle[\hat{\Phi}_\alpha^\dagger(\mathbf{r}_\perp)\hat{\Phi}_\alpha(\mathbf{r}_\perp)]^2\rangle$ where the z dependence in the expectation values is integrated out. In the spin-1 case analyzed here, we observe within the HFP approximation that the fraction of the component with suppressed total density fluctuations given by $\int d\mathbf{r}_\perp \sqrt{\mathcal{C}(\mathbf{r}_\perp)}/N_{\text{tot}}$, decreases very slowly with increasing temperature. This illustrates the role of the thermally induced intercomponent density fluctuations.

We determine the quasicondensate component by considering the total density fluctuations restricted to the c-field region and define the quasicondensate density as

$$n_{qc}(\mathbf{r}) = \sqrt{2\langle|\bar{\Psi}_c(\mathbf{r})|^2\rangle^2 - \langle|\bar{\Psi}_c(\mathbf{r})|^4\rangle}. \quad (11)$$

For the parameters discussed in Section III, the c field is of the form $\bar{\Psi}_c(\mathbf{r}) = \bar{\Psi}_c(\mathbf{r}_\perp)\varphi_0(z)$, where $\varphi_0(z)$ is the lowest harmonic oscillator state. Hence, the z dependence in $n_{qc}(\mathbf{r})$ can be integrated out. The quasicondensate fraction is shown in Fig. 2 and it persists at the temperatures where the condensate fraction becomes negligible. The critical temperature for the formation of the coherent condensate as well as the onset of the quasicondensate are the same for the in-plane and the out-of-plane nematic phases, and they take place at temperatures $T' = 0.97 \pm 0.02$ and $T' = 1.16 \pm 0.04$, respectively (from Fig. 2). In addition, the quasicondensate fraction is essentially the same at equal temperatures in both cases. Due to the reduced total density fluctuations at all temperatures, the quasi-condensate component is delocalized to the entire spatial extent of the c-field atoms whereas the condensate com-

ponent tends to be localized to the region where HQVs and skyrmions are rare (see Fig. 1).

Since the reduced temperature for the onset of a condensate is the same for both nematic phases within the numerical accuracy, it is natural to ask if it is caused by the condensate depletion due to the incoherent atoms. Although the number of the incoherent region atoms is large near the onset of the condensate, the same onset temperature for the condensate is found if only the c-field atoms are taken into account. In Fig. 3, the fraction N_0/N_C is shown as a function of the reduced temperature, indicating that the onset of a large eigenvalue takes place at equal temperatures for both nematic phases. Hence, the onset of a nonzero condensate fraction at the same temperature for both nematic phases does not depend on the depletion of the condensate due to the incoherent region atoms.

V. PROLIFERATION OF TOPOLOGICAL DEFECTS

In trapped atomic gases, the characteristic feature of the crossover from a BKT type of superfluid to a normal fluid is a proliferation and a subsequent propagation of free vortices from the edge of the cloud to the central region of the trap. Since HQVs are nonsingular defects, they persist at the edge of the cloud to relatively low temperatures (Fig. 1) and the system can be considered to have concentric shells of normal fluid and BKT superfluid with the center of the trap occupied by the condensate. We analyze the BKT crossover by studying the HQV occupation probability density P_r [14]. An estimate for the crossover temperature is obtained from the temperature at which P_r becomes nonzero near the center of the trap (see Fig. 4). From this analysis, the BKT crossover takes place roughly at the reduced temperature $T'_{\text{BKT}} = 0.82 \pm 0.05$ for the in-plane nematic and at $T'_{\text{BKT}} = 0.89 \pm 0.04$ for the out-of-plane nematic phase.

Since the reduced BKT crossover temperature obtained previously has a rather large uncertainty, we cannot conclusively determine the relation between the crossover temperatures for the two nematic phases. However, since the order parameter has a different symmetry in the in-plane and out-of-plane phases, there is no reason to assume that the crossover temperature is the same. For the in-plane nematic phase the symmetry is reduced to $[U(1) \times S^1]/\mathbb{Z}_2$ while in the case of an out-of-plane nematic it is $[U(1) \times S^2]/\mathbb{Z}_2$, allowing the existence of skyrmions which in the homogeneous case render the system spin-disordered. In a finite-size system, the thermal activation of skyrmions depends on the characteristic size of skyrmions compared to that of the system, and we find that skyrmions start to appear only at relatively high temperatures near the BKT crossover, see Fig. 4.

The effect of skyrmions to the crossover temperature T_{BKT} can be illustrated by considering the statistical probability for the activation of a skyrmion or a pair of HQVs. The probability is proportional to the Boltzmann factor $\exp(-\Delta\mathcal{F}/k_B T)$ where $\Delta\mathcal{F} = \Delta\mathcal{E} - T\Delta S$ is the free-energy change associated with the creation of a given defect. The critical temperature for the activation of different defects can be estimated from the condition $\Delta\mathcal{F} = 0$. In a uniform 2D system, the en-

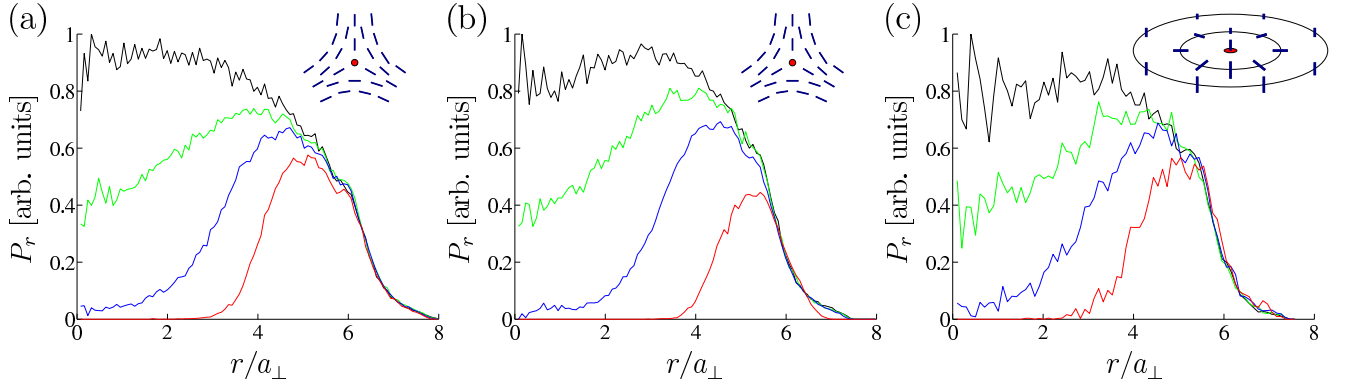


Figure 4: (Color online) Radial probability density for detecting (a) a HQV in the in-plane nematic, (b) a HQV in the out-of-plane nematic, and (c) a skyrmion in the out-of-plane nematic phase. The reduced temperatures are given by (from top to bottom in each panel) 1.05, 0.95, 0.82, 0.63 in (a), 1.00, 0.94, 0.89, 0.64 in (b), and 1.00, 0.96, 0.92, 0.84 in (c).

entropy change associated with the creation of a skyrmion can be approximately evaluated as [6, 7, 62] $\Delta S_{\text{sk}} = 2k_B \ln(\ell/r_0)$ where ℓ is the linear size of the system and r_0 the characteristic size of a skyrmion. The skyrmion energy $\mathcal{E}_{\text{sk}} = 4\pi\hbar^2 \rho/m$ is finite and independent of the size of the skyrmion (see Appendix). Hence, the free energy is always negative for a large enough system and skyrmions exist at all temperatures in the thermodynamical limit [63].

Since the BKT transition is driven by the dissociation of bound pairs of vortices and antivortices [64], we estimate the critical temperature using the Boltzmann probability for the appearance of free vortices [6, 7]. In the Appendix, the energy of a free HQV is shown to be $\mathcal{E}_{\text{HQV}} = \frac{\pi\hbar^2 \rho}{2m} \ln(\ell/r_1)$, where r_1 is the size of the HQV core. The corresponding entropy change is $\Delta S_{\text{HQV}} = 2k_B \ln(\eta\ell/r_1)$, where $\eta < 1$ in the presence of skyrmions due to screening. This would result in a higher critical temperature for the activation of free HQVs in the out-of-plane nematic phase where skyrmions are allowed. In nonuniform finite-size systems, the mechanism is different since the skyrmions appear only near T_{BKT} . The thermal fluctuations generate skyrmions first at the boundary of the cloud and since the skyrmion energy is independent of its size, this process is not strongly affected by the pre-existing HQVs. The generation of skyrmions can prevent the thermal fluctuations from breaking the HQV–anti-HQV pairs, thereby giving rise to the higher crossover temperature.

The crossover temperature can also be studied using the 2D phase-space density $\bar{n}_c^{(2D)} \lambda^2$, where $\bar{n}_c^{(2D)}$ is the average 2D total density of the c-field atoms at $r_\perp = 0$ and $\lambda = \sqrt{2\pi\hbar^2/mk_B T}$. We observe that the phase-space density takes roughly the value 25 for both nematic phases at the respective reduced crossover temperatures (see Fig. 5). This result is to be contrasted with the single-component case where the transition to the superfluid phase takes place when the phase-space density is larger than the critical value

$$\bar{n}_{\text{crit}}^{(2D)} \lambda^2 = \ln(C/\tilde{g}), \quad (12)$$

where $\tilde{g} = \sqrt{8\pi} a/a_z$, a is the s -wave scattering length in the single component system, and $C \approx 380$ [15, 61]. For

the spin-1 system considered here, the corresponding 2D coupling constants can be defined as $\tilde{c}_0 = \sqrt{8\pi}(a_0 + 2a_2)/3a_z$ and $\tilde{c}_2 = \sqrt{8\pi}(a_2 - a_0)/3a_z$. The parameters defined in Sec. II yield $\tilde{c}_0 = 0.028$ and $\tilde{c}_2 = 0.0011$. The value of \tilde{c}_0 is comparable to the experimental value $\tilde{g} = 0.02$ in the single-component system of Ref. [13] where the spin-dependent interaction is absent. A simple-minded application of the scalar case condition (12) using either of the coupling constants \tilde{c}_0 and \tilde{c}_2 with $C = 380$ yields much lower values than $\bar{n}_c^{(2D)} \lambda^2 = 25$. This suggests that if a condition analogous to Eq. (12) exists for the spinor case, its form is different from (12).

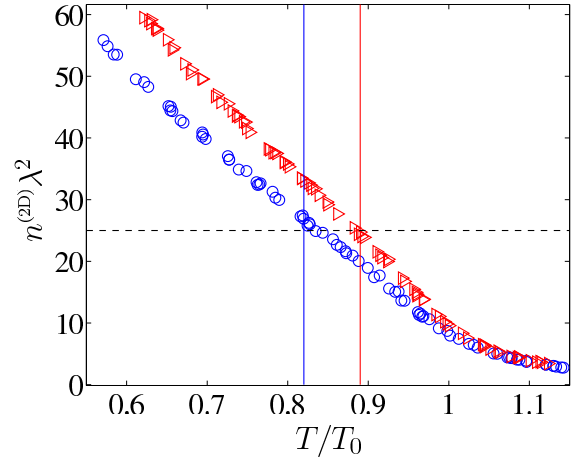


Figure 5: (Color online) The phase-space density $\bar{n}_c^{(2D)} \lambda^2$ as function of the reduced temperature for the in-plane nematic (blue circles) and out-of-plane nematic (red triangles). The solid lines denote the BKT crossover temperatures $T_{\text{BKT}}' = 0.82$ and $T_{\text{BKT}}' = 0.89$ for the in-plane and the out-of-plane nematic phases, respectively. The dashed line corresponds to the phase-space density $\bar{n}_{\text{crit}}^{(2D)} \lambda^2 = 25$.

An important check for the observed crossover temperatures is the superfluid density which is predicted to change in the spinor case noncontinuously across the phase transition

by the amount [26]

$$\Delta\rho_s = 8m^2k_B T_{\text{BKT}}/(\pi\hbar^2). \quad (13)$$

Hence, the universal jump in the superfluid density is four times larger than in the single-component case. To use this property to check the consistency of the crossover temperatures, an independent computation of the superfluid density is required. Since the system is inhomogeneous, the central part of the system is typically in the superfluid state while the outer part corresponds to normal fluid. This renders methods such as the computation of the helicity modulus [26, 65] inapplicable since they require a uniform system without coexisting phases.

The HQVs are nonsingular vortices and the nonclassical moment of inertia [12] does not capture the BKT crossover. The phenomenological models for the trapped systems in the single-component case [12, 15] make use of the condition (12) and assume explicitly a sudden change in the superfluid density by the universal value $2m^2k_B T_{\text{BKT}}/(\pi\hbar^2)$. Hence, there is a clear incentive for further investigations of the superfluid properties of spinor Bose gases, in particular for the determination of the superfluid fraction without making use of Eq. (13). We note that the condition $\bar{n}_{\text{crit}}^{(2\text{D})}\lambda^2 = 25$ is consistent with Eq. (13) since the crossover temperature yields $(\rho_s = mn_s)n_s/\bar{n}_{\text{crit}}^{(2\text{D})} = 0.64$. Using the scalar condition (12) with \tilde{g} equal to either \tilde{c}_0 or \tilde{c}_2 gives $n_s/\bar{n}_{\text{crit}}^{(2\text{D})} > 1$, indicating that the scalar condition (12) is not valid for the spinor case.

We note that the uncertainty in the determination of the BKT crossover temperature in terms of the reduced temperature T_{BKT}/T_0 allows in principle the crossover temperature to be the same for both nematic phases. However, if there is a critical value for the phase-space density independent of the type of the nematic ordering, then the data in Fig. 5 yield different reduced crossover temperatures if they are below the condensation temperature $T' \approx 0.97$. We also note that it is numerically difficult to distinguish between skyrmions and merons when there are large fluctuations in the direction of the magnetic axis $\hat{n}(r_\perp)$, but in an analogy to the homogeneous 2D situation, we refer to these out-of-plane defects as skyrmions. In the in-plane case, skyrmions are not allowed but, instead, integer vortices corresponding to winding 2π of in the magnetic axis around the vortex core can take place. Such vortices seem to remain suppressed suggesting that they are irrelevant for the BKT crossover.

VI. DISCUSSION

We have analyzed the realization of the BKT transition in antiferromagnetic spin-1 Bose gases under typical experimental conditions. We have found a hierarchy of crossover temperatures corresponding to the onset of a quasicondensate at a high temperature and the formation of a coherent condensate at a lower temperature, followed by a BKT-type of crossover to a superfluid state as the temperature decreases. The investigation of the probability density for the excitation of skyrmions and half-quantum vortices did not unequivocally

determine the relation between nematic ordering and the magnitude of the crossover temperature. The subsequent inspection of the 2D phase-space density at the center of the trap suggested that the crossover temperature expressed in terms of the reduced temperature could be slightly higher for the out-of-plane phase. Further investigations are still needed to confirm this scenario. The finite size of the system is manifested as a finite activation temperature for the skyrmions and the thermal fluctuations start to generate skyrmions only near the crossover temperature. It remains an open question if another crossover to a fragmented condensate takes place in the zero-temperature limit.

We expect that the fractional population of different Zeeman sublevels can be controlled using rf pulses and magnetic-field gradients [66] to allow the experimental realization of the in-plane and the out-of-plane nematic phases. Using the time-of-flight imaging combined to the Stern-Gerlach separation of the different Zeeman sublevels, formation of the condensate component can be observed. The ferromagnetic cores of the HQVs could be detected by imaging the magnetization of the gas [37, 66] and the same technique can in principle be extended to image directly also the spin quadrupole order [36, 37, 67]. Interference experiments [10] can also be useful to demonstrate the existence of free vortices around the BKT crossover temperature.

Acknowledgments

The authors acknowledge the Jenny and Antti Wihuri Foundation, the Emil Aaltonen Foundation, the Japan Society for the Promotion of Science (JSPS), and the Academy of Finland for financial support and the Center for Scientific Computing Finland (CSC) for computing resources.

Part of this research was carried out in the Centre for Quantum Computer Technology supported by the Australian Research Council, the Australian Government, the U.S. National Security Agency (NSA), and the U.S. Army Research Office (ARO) (under Contract No. W911NF-08-1-0527).

Appendix: Energies of skyrmions and HQV–anti-HQV pairs in uniform systems

The skyrmion configuration can be represented on a Cartesian basis such that $\vec{\Psi} = \sqrt{\varrho}e^{i\theta}\hat{n}$, with

$$\hat{n} = (\sin\beta(\rho)\cos\varphi, \sin\beta(\rho)\sin\varphi, \cos\beta(\rho)), \quad (\text{A.1})$$

where (ρ, φ) denote the polar coordinates and function $\beta(\rho)$ satisfies the boundary conditions $\beta(0) = 0$ and $\beta(\rho) = \pi$ for $\rho > r_0$. A meron (half-skyrmion) is obtained with $\beta(\rho) = \pi/2$ for $\rho > r_0$. We assume a uniform system such that the density ϱ is a constant for skyrmions and HQVs. For the skyrmion configuration (A.1), the $U(1)$ phase θ can be taken to be a constant.

The low-energy theory for the polar phase is the nonlinear

σ model (NL σ M) of the form [26]

$$\mathcal{L} = \frac{K}{2} \int d\mathbf{r}_\perp [(\nabla\hat{\mathbf{n}})^2 + (\nabla\theta)^2], \quad (\text{A.2})$$

where the superfluid stiffness is $K = \hbar^2 \rho/m$. The NL σ M has a conformal invariance such that the energy of a skyrmion can become independent of the size r_0 . Furthermore, all configurations of the form (A.1) satisfy the condition $\mathcal{E}_{\text{sk}} \geq 4\pi K$ [63]. Hence we can take the energy of the skyrmion to be $\mathcal{E}_{\text{sk}} = 4\pi K$.

Outside the vortex core for $\rho > r_1$, the HQV configuration corresponds to $\theta = \varphi/2$ and

$$\hat{\mathbf{n}} = \left(\cos \frac{\varphi}{2}, \sin \frac{\varphi}{2}, 0 \right). \quad (\text{A.3})$$

Assuming that the systems has linear size ℓ , substitution of (A.3) into (A.2) yields the energy $\mathcal{E}_{\text{HQV}} = \frac{\pi K}{2} \ln(\ell/r_1)$. The HQV energy does not include the contribution from the vortex core which is negligible in the thermodynamical limit. Furthermore, the usual arguments [59] can be used to conclude that the energy of a HQV–anti-HQV pair is in the leading order $\mathcal{E}_{\text{PHQV}} = \pi K \ln(d/r_1)$, where d is the distance between the vortex cores.

-
- [1] N. D. Mermin and H. Wagner, *Phys. Rev. Lett.* **17**, 1133 (1966).
[2] P. C. Hohenberg, *Phys. Rev.* **158**, 383 (1967).
[3] S. Coleman, *Commun. Math. Phys.* **31**, 259 (1973).
[4] V. L. Berezinskii, *Sov. Phys. JETP* **32**, 493 (1971).
[5] V. L. Berezinskii, *Sov. Phys. JETP* **34**, 610 (1972).
[6] J. M. Kosterlitz and D. J. Thouless, *J. Phys. C* **5**, L124 (1972).
[7] J. M. Kosterlitz and D. J. Thouless, *J. Phys. C* **6**, 1181 (1973).
[8] S. T. Bramwell and P. C. W. Holdsworth, *J. Phys.: Condens. Matter* **5**, 53 (1993).
[9] T. P. Simula and P. B. Blakie, *Phys. Rev. Lett.* **96**, 020404 (2006).
[10] Z. Hadzibabic, P. Krüger, M. Cheneau, B. Battelier, and J. Dalibard, *Nature* **441**, 1118 (2006).
[11] V. Schweikhard, S. Tung, and E. A. Cornell, *Phys. Rev. Lett.* **99**, 030401 (2007).
[12] M. Holzmann and W. Krauth, *Phys. Rev. Lett.* **100**, 190402 (2008).
[13] P. Cladé, C. Ryu, A. Ramanathan, K. Helmerson, and W. D. Phillips, *Phys. Rev. Lett.* **102**, 170401 (2009).
[14] T. P. Simula, M. J. Davis, and P. B. Blakie, *Phys. Rev. A* **77**, 023618 (2008).
[15] R. N. Bisset, M. J. Davis, T. P. Simula, and P. B. Blakie, *Phys. Rev. A* **79**, 033626 (2009).
[16] T. Ohmi and K. Machida, *J. Phys. Soc. Jpn.* **67**, 1822 (1998).
[17] T.-L. Ho, *Phys. Rev. Lett.* **81**, 742 (1998).
[18] J. Stenger, S. Inouye, D. M. Stamper-Kurn, H.-J. Miesner, A. P. Chikkatur, and W. Ketterle, *Nature* **396**, 345 (1998).
[19] T.-L. Ho and S. K. Yip, *Phys. Rev. Lett.* **84**, 4031 (2000).
[20] U. Leonhardt and G. E. Volovik, *JETP. Lett.* **72**, 66 (2000).
[21] E. Demler and F. Zhou, *Phys. Rev. Lett.* **88**, 163001 (2002).
[22] A.-C. Ji, W. M. Liu, J. L. Song, and F. Zhou, *Phys. Rev. Lett.* **101**, 010402 (2008).
[23] K. C. Wright, L. S. Leslie, A. Hansen, and N. P. Bigelow, *Phys. Rev. Lett.* **102**, 030405 (2009).
[24] J. L. Song and F. Zhou, *Europhys. Lett.* **85**, 20002 (2009).
[25] D. Podolsky, S. Chandrasekharan, and A. Vishwanath, *Phys. Rev. B* **80**, 214513 (2009).
[26] S. Mukerjee, C. Xu, and J. E. Moore, *Phys. Rev. Lett.* **97**, 120406 (2006).
[27] S. Hoshi and H. Saito, *Phys. Rev. A* **78**, 053618 (2008).
[28] M. M. Salomaa and G. E. Volovik, *Phys. Rev. Lett.* **55**, 1184 (1985).
[29] E. Babaev, *Nucl. Phys. B* **686**, 397 (2004).
[30] E. Babaev, *Phys. Rev. Lett.* **94**, 137001 (2005).
[31] S. B. Chung, H. Bluhm, and E.-A. Kim, *Phys. Rev. Lett.* **99**, 197002 (2007).
[32] K. G. Lagoudakis, T. Ostatnický, A. V. Kavokin, Y. G. Rubo, R. André, and B. Deveaud-Plédran, *Science* **326**, 974 (2009).
[33] Y. Liu, S. Jung, S. E. Maxwell, L. D. Turner, E. Tiesinga, and P. D. Lett, *Phys. Rev. Lett.* **102**, 125301 (2009).
[34] Y. Liu, E. Gomez, S. E. Maxwell, L. D. Turner, E. Tiesinga, and P. D. Lett, *Phys. Rev. Lett.* **102**, 225301 (2009).
[35] C.-L. Hung, X. Zhang, N. Gemelke, and C. Chin, *Phys. Rev. A* **78**, 011604(R) (2008).
[36] I. Carusotto and E. J. Mueller, *J. Phys. B.: At. Mol. Opt. Phys.* **37**, S115 (2004).
[37] J. M. Higbie, L. E. Sadler, S. Inouye, A. P. Chikkatur, S. R. Leslie, K. L. Moore, V. Savalli, and D. M. Stamper-Kurn, *Phys. Rev. Lett.* **95**, 050401 (2005).
[38] P. B. Blakie, A. S. Bradley, M. J. Davis, R. J. Ballagh, and C. W. Gardiner, *Adv. Phys.* **57**, 363 (2008).
[39] R. N. Bisset and P. B. Blakie, *Phys. Rev. A* **80**, 035602 (2009).
[40] M. J. Davis, S. A. Morgan, and K. Burnett, *Phys. Rev. Lett.* **87**, 160402 (2001).
[41] M. J. Davis and S. A. Morgan, *Phys. Rev. A* **68**, 053615 (2003).
[42] M. J. Davis and P. B. Blakie, *Phys. Rev. Lett.* **96**, 060404 (2006).
[43] P. B. Blakie and M. J. Davis, *J. Phys. B: At. Mol. Opt. Phys.* **40**, 2043 (2007).
[44] A. Bezett, E. Toth, and P. B. Blakie, *Phys. Rev. A* **77**, 023602 (2008).
[45] A. Bezett and P. B. Blakie, *Phys. Rev. A* **79**, 033611 (2009).
[46] T. Sato, T. Suzuki, and N. Kawashima, *J. Phys.: Conf. Ser.* **150**, 032094 (2009).
[47] K. Gawryluk, M. Brewczyk, M. Gajda, and K. Rzążewski, *Phys. Rev. A* **76**, 013616 (2007).
[48] D. S. Petrov, M. Holzmann, and G. V. Shlyapnikov, *Phys. Rev. Lett.* **84**, 2551 (2000).
[49] I. Bloch, M. Dalibard, and W. Zwerger, *Rev. Mod. Phys.* **80**, 855 (2008).
[50] M. J. Davis and P. B. Blakie, *J. Phys. A: Math. Gen.* **38**, 10259 (2005).
[51] H. H. Rugh, *Phys. Rev. Lett.* **78**, 772 (1997).
[52] H. H. Rugh, *Phys. Rev. E* **64**, 055101(R) (2001).
[53] W. Zhang, S. Yi, and L. You, *Phys. Rev. A* **70**, 043611 (2004).
[54] E. J. Mueller, *Phys. Rev. A* **69**, 033606 (2004).

- [55] F. Zhou, Phys. Rev. Lett. **87**, 080401 (2001).
- [56] F. Zhou, Int. J. Mod. Phys. **B17**, 2643 (2003).
- [57] L. Santos, M. Fattori, J. Stuhler, and T. Pfau, Phys. Rev. A **75**, 053606 (2007).
- [58] P. B. Blakie, Phys. Rev. E **78**, 026704 (2008).
- [59] L. Pitaevskii and S. Stringari, *Bose-Einstein Condensation* (Oxford University Press, Oxford, 2003).
- [60] E. J. Mueller, T. L. Ho, M. Ueda, and G. Baym, Phys. Rev. A **74**, 033612 (2006).
- [61] N. Prokof'ev, O. Ruebenacker, and B. V. Svistunov, Phys. Rev. Lett. **87**, 270402 (2001).
- [62] T. P. Simula, M. D. Lee, and D. A. W. Hutchinson, Phil. Mag. Lett. **85**, 395 (2005).
- [63] A. A. Belavin and A. M. Polyakov, JETP. Lett. **22**, 245 (1975).
- [64] A. N. Berker and D. R. Nelson, Phys. Rev. B **19**, 2488 (1979).
- [65] M. E. Fisher, M. N. Barber, and D. Jasnow, Phys. Rev. A **8**, 1111 (1973).
- [66] M. Vengalattore, J. Guzman, S. Leslie, F. Serwane, and D. M. Stamper-Kurn (2009), arXiv:0901.3800.
- [67] H. Chiba and H. Saito, Phys. Rev. A **78**, 043602 (2008).